Journal Pre-proofs

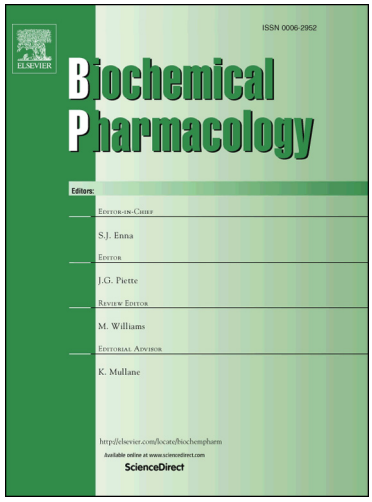

The cardenolides ouabain and reevesioside A promote FGF2 secretion and subsequent FGFR1 phosphorylation via converged ERK1/2 activation

Guan-Hao Zhao, Ya-Qi Qiu, Cheng-Wei Yang, Ih-Sheng Chen, Chin-Yu Chen, Shiow-Ju Lee

PII: S0006-2952(19)30440-X
DOI: https://doi.org/10.1016/j.bcp.2019.113741
Reference: BCP 113741

To appear in: *Biochemical Pharmacology*

Received Date: 10 September 2019
Accepted Date: 2 December 2019

Please cite this article as: G-H. Zhao, Y-Q. Qiu, C-W. Yang, I-S. Chen, C-Y. Chen, S-J. Lee, The cardenolides ouabain and reevesioside A promote FGF2 secretion and subsequent FGFR1 phosphorylation via converged ERK1/2 activation, *Biochemical Pharmacology* (2019), doi: https://doi.org/10.1016/j.bcp.2019.113741

The cardenolides ouabain and reevesioside A promote FGF2 secretion and subsequent FGFR1 phosphorylation via converged ERK1/2 activation

Guan-Hao Zhao[1,3], Ya-Qi Qiu[1], Cheng-Wei Yang[1], Ih-Sheng Chen[2], Chin-Yu Chen[3], Shiow-Ju Lee*[1]

[1]Institute of Biotechnology and Pharmaceutical Research, National Health Research Institutes, Miaoli 35053, Taiwan, ROC.

[2] School of Pharmacy, College of Pharmacy, Kaohsiung Medical University, Kaohsiung, Taiwan, ROC.

[3] Department of Life Sciences, National Central University, Taoyuan 32001, Taiwan ROC.

*To whom correspondence should be addressed. Tel: +886-37-246166 ext. 35715; Fax: +886-37-586456; Email: slee@nhri.org.tw

Running title: Cardenolides activate ERK1/2 to promote FGF2 secretion and FGFR1 activation

Highlights:

1) Cardenolides induced FGF2 secretion and FGFR1 phosphorylation in A549 cells.
2) Cardenolide ouabain triggered the EGFR associated ERK 1/2 activation.
3) Cardenolide ouabain diminished the MKP1 protein level and thus resulted in ERK 1/2 activation.
4) Cardenolides induced converged ERK1/2 activation to promote the FGF2 export in A549 cells.

Abstract:

Na^+/K^+-ATPase α1 was reported to directly interact with and recruit FGF2 (fibroblast growth factor 2), a vital cell signaling protein implicated in angiogenesis, to the inner plasma membrane for subsequent secretion. Cardenolides, a class of cardiac glycosides, were reported to downregulate FGF2 secretion upon binding to Na^+/K^+-ATPase α1 in a cell system with ectopically expressed FGF2 and Na^+/K^+-ATPase α1. Herein, we disclose that the cardenolides ouabain and reevesioside A significantly enhance the secretion/release of FGF2 and the phosphorylation of FGFR1 (fibroblast growth factor receptor 1) in a time- and dose-dependent manner, in A549 carcinoma cells. A pharmacological approach was used to elucidate the pertinent upstream effectors. Only the ERK1/2 inhibitor U0126 but not the other inhibitors examined (including those inhibiting the unconventional secretion of FGF2) was able to reduce ouabain-induced FGF2 secretion and FGFR1 activation. ERK1/2 phosphorylation was increased upon ouabain treatment, a process found to be mediated through upstream effectors including ouabain-induced phosphorylated EGFR and a reduced MKP1 protein level. Therefore, at least two independent lines of upstream effectors are able to mediate ouabain-induced ERK1/2 phosphorylation and the subsequent FGF2 secretion and FGFR1 activation. These finding constitute unprecedent insights into the regulation of FGF2 secretion by cardenolides.

Key words: EGFR; ERK1/2; FGF2; MKP1; Na^+/K^+-ATPase α1; ouabain.

1. Introduction

Basic fibroblast growth factor (bFGF/FGF2) is an endocrine growth factor and signaling protein that plays a vital role in angiogenesis. FGF2 lacks a signal peptide sequence for the classic protein secretion through the ER/Golgi process and is instead secreted in an unconventional route (Florkiewicz et al., 1995; Zacherl et al., 2015) which has been reported in the context of: 1) potentially unassembled α1-chains of Na^+/K^+-ATPase for FGF2 recruitment at the inner leaflet of plasma membranes; 2) Tec kinase-mediated phosphorylation of FGF2; 3) phosphatidylinositol 4,5-bisphosphate-dependent membrane translocation of FGF2; and 4) extracellular heparan sulfate proteoglycans for completing of FGF2 membrane translocation (Ebert et al., 2010; Florkiewicz et al., 1998; Nickel, 2007, 2011; Nickel and Seedorf, 2008; Zacherl et al., 2015).

The FGFR (fibroblast growth factor receptor) family comprises four distinct members, FGFR1 to FGFR4, all of which possess tyrosine kinase activity. However, their expression levels are tissue-specific (Itoh and Ornitz, 2004; Wilkie et al., 1995), and therefore the specificities and selectivities of their ligand binding are anticipated to be very different. Over 20 divergent FGF (fibroblast growth factor) families have been identified (Ornitz and Itoh, 2001), and they regulate multiple cellular processes through binding to FGFRs (Ornitz and Itoh, 2015). Upon FGF binding to its specific FGFR, the FGFR dimerizes, its tyrosine sites in the intracellular domain are auto-phosphorylated, and it becomes active (Ornitz and Itoh, 2015). Subsequently, the active FGF/FGFR -triggers downstream signaling, whereupon it is internalized through endocytosis and

degraded, resulting in signaling termination (Wesche et al., 2011). FGF/FGFR signaling is involved in cell growth, migration, and differentiation in critical development, and also affects metabolism, repair, regeneration and wound healing in adult tissues (Coumoul and Deng, 2003; Du et al., 2012; Hogan et al., 2014).

Functional Na^+/K^+-ATPase consists of a catalytic α subunit and two regulatory subunits (one β and one γ), and pumps two K^+ into cells for every three Na^+ that are pumped out (Baker Bechmann et al., 2016; Diederich et al., 2017; Katz et al., 2015). The unassembled α1-chain of Na^+/K^+-ATPase was reported to directly interact with the FGF2 through its intracellular domain, thereby recruiting FGF2 to the inner plasma membrane for subsequent secretion; whereas the β subunit is dispensable, for the purpose of FGF2 secretion (Dahl et al., 2000; Florkiewicz et al., 1998; Zacherl et al., 2015). The cardenolides, a class of cardiac glycosides, were reported to inhibit FGF2 export through binding to the unassembled α1-chain of Na^+/K^+-ATPase at the cell surface in transfected primate cells, e.g. COS-1; CV-1, with expression vectors of FGF2 or α1-chain of Na^+/K^+-ATPase (Dahl et al., 2000; Florkiewicz et al., 1998). Conventionally, cardenolides bind to functional Na^+/K^+-ATPase through multi-interactions within the α subunit, causing the Na^+/K^+-ATPase complex to undergo a conformational change, inhibiting its membrane potential generating function (Laursen et al., 2013). However, under endogenous expressed FGF2 and Na^+/K^+-ATPase α1, it is still unclear whether (i) FGF2 binds to unassembled or functional complexed Na^+/K^+-ATPase α1 subunit, for recruitment to the inner membrane for secretion, and (ii) whether cardenolides inhibit FGF2 secretion by binding to

the functional Na^+/K^+-ATPase complex, or to the unassembled Na^+/K^+-ATPase $\alpha 1$ subunit.

Herein, we disclose that the cardenolides ouabain and reevesioside A, significantly enhanced the secretion/release of FGF2 to culture medium, and in turn to activated FGFR1 in carcinoma A549 cells. We further demonstrated that, upon ouabain treatment, at least two independent signaling axes were triggered for ERK1/2 activation, resulting in enhanced FGF2 secretion and FGFR1 activation. These findings provide unprecedented insights into the endogenous pathways for the regulation of FGF2 secretion by cardenolides.

2. Materials and Methods

2.1 Reagents

Reevesioside A was prepared and obtained as previously described (Chang et al., 2013a) and its purity was determined ($\geqq$95%, HPLC) as described (Lee et al., 2012). Ouabain (Cat # O3125, $\geqq$ 95%, HPLC), digoxin (Cat # D6003, $\geqq$95%, HPLC), NSC95397 (Cat # N1786, $\geqq$97%, HPLC), and methylamine solution (MeNH2; Cat # 395048, 2.0 M in MeOH), were purchased from Sigma-Aldrich (St. Louis, MO, USA). SU5402 (Cat # 572630, $\geqq$95%, HPLC) and MG132 (Cat # 474790, $\geqq$98%, HPLC) were purchased from Calbiochem (San Diego, CA, USA) . LFM-A13 (Cat # S7734, $\geqq$ 99.7%, HPLC) was purchased from Selleckchem (Karl-Schmid-Str. 14, Munich, Germany). U0126 (Cat # PHZ1283, 95%, TLC) and LY294002 (Cat # PHZ1144, 99%, TLC) were

purchased from ThermoFisher (Waltham, MA, USA). Gefitinib (Cat # 13166, ≧ 98%) was purchased from Cayman Chemical (Ann Arbor, MI, USA). CellTiter 96® AQueous MTS Reagent Powder and phenazine methosulfate (PMS) solution were purchased from Promega (Madison, WI, USA).

2.2 Cell culture

A549 carcinoma cell lines (BCRC 60074) were obtained from Bioresource Collection and Research Center (BCRC) and passaged within six months of receipt, and further established as stock in the cell bank at early passage to ensure cell line-specific characteristics (Hughes et al., 2007). The passage 8 to 15 were used in this study. The procedures for cell culture were carried out as described previously (Qiu et al., 2015) with the following modification: cells were cultured and maintained in RPMI-1640 medium (GIBCO-Life Technologies) with 10% fetal bovine serum (FBS; Hyclone Laboratory Inc.) and 1% Penicillin/Streptomycin (P/S; Biological Industries) in a humidified incubator of 5% CO_2 atmosphere at 37 °C. For compound treatment studies, cells were then incubated in serum starved conditions with RPMI-1640 culture medium containing only 1% FBS.

2.3 Cell cytotoxicity and drug combination assays

We used drug combination assays and isobologram analyses to assess the interaction between SU5402, a FGFR1 inhibitor, and cardenolides. The A549 cells were seeded into 96-well plates at a

density of 3000 cells/well and subjected to overnight growth. Both SU5402 and cardenolides were subjected to a series of two-fold dilutions from the indicated higher and lower concentration in drug combination assays. The inhibitory concentration at 50% growth (IC_{50}) of SU5402 and reevesioside A were determined alone. The IC_{50} values of combined treatments were measured at the concentrations below their IC_{50} values in the isobologram analysis. The drug effects on cell growth inhibition were estimated by MTS assay after 72 hr of treatment by the combined MTS/PMS solution; and the absorbances at 490 nm were recorded after incubation. The IC_{50} values were calculated by the linear interpolation method between two data points above and below 50% inhibition. Combination index (CI) values were estimated using the software program CalcuSyn (Biosoft); for ED values below 0.8, a synergistic effect is inferred; for those between 0.8 and 1.2 an additive effect, and those above 1.2 an antagonistic effect. In the isobologram analysis, the additive effect is depicted as a straight line, plotted between the IC_{50} values of SU5402 or reevesioside A treatment alone. Doses of each drug used in combination treatments that when plotted lie to the left and below the additive plot correspond to a synergistic effect; whereas those that lie on the opposite side correspond to an antagonistic effect.

2.4 Western analyses

A549 cells were seeded into six-well plates at a density of 10^6 cells/well one day before treatment. Cells were harvested and lysed in lysis buffer (1% NP40, 50 mM Tris-HCl [pH7.5], 300 mM NaCl, 5

mM EDTA) containing 2 mM phenylmethylsulfonyl fluoride (PMSF), 2 mM sodium orthovanadate (Na_3VO_4), 10 mM sodium fluoride (NaF) and complete EDTA free protease inhibitor cocktail (Roche). Equal amounts of protein were denatured in protein loading buffer (GeneMark), subjected to sodium dodecyl sulfate-polyacrylamide gel electrophoresis (SDS-PAGE), transferred to nitrocellulose (NC) membranes (GE Healthcare) in ice-cold tris/glycine transfer buffer containing 10% (v/v) ethanol (EtOH), probed with indicated primary antibodies in blocking buffer, and followed by detection with a horseradish peroxidase (HRP)-linked secondary antibodies, Western Lightning Plus (PerkinElmer Life Sciences) and x-ray film (Roche). The primary antibodies used in this study were as follows: FGF2 (Santa Cruz, Cat # sc-79, Lot # D0704), phospho-FGFR1 (Y766; Cell Signaling, Cat # 2544, Lot # 2), FGFR1 (Cell Signaling, Cat # 9740, Lot # 4), phospho-ERK1/2 (T202/Y204; Cell Signaling, Cat # 4370, Lot # 12), ERK1/2 (Thermo, Cat # 44-654G, Lot # 0601), phospho-JNK (T183/Y185; Cell Signaling, Cat # 9251, Lot # 17), JNK (Cell Signaling, Cat # 9252, Lot # 5), active p38 (pTGpY; Promaga, Cat # V1211), p38 (Biosource, clone # 2F11, Cat # AHO0782, Lot # 20505-01R), GAPDH (Cell Signaling, Cat # 2118, Lot # 10), MKP1 (sc-370, Santa Cruz, Lot # L0910) , phospho-EGFR (Y845; Cell signaling, Cat # 2231, Lot # 8), EGFR (GeneTex, Cat # 100448, Lot # 39645), Na^+/K^+-ATPase $\alpha 1$ (Abcam, clone # 464.6, Cat # ab7671, Lot # GR161548-6). Enhanced chemiluminescence detection reagents (Western Blot Chemiluminescence Reagent Plus; PerkinElmer) were used to detect antigen–antibody complexes according to the manufacturers' instructions. Relative protein levels were estimated and normalized with GAPDH or

as indicated using a ScanMaker E900 scanner (600 dpi) to scan the western films, and quantitated by Image-J software. The multiple bands occurred to some proteins that represent their isoforms with different sizes or differential posttranslational modifications which cause in the different motility in the SDS- PAGE/western blot. All these bands we detected are as shown in their respective manufacturer's antibody-data sheet corresponding to their category number provided above or as reported(Lee et al., 2005; Pinilla-Macua et al., 2017).

2.5 Enzyme-linked immunosorbent assay

Culture supernatants were collected and centrifuged at 1000 g for 5 min to remove particulates. Fibroblast growth factor 2 (FGF2) ELISA kits were purchased from R&D Systems and the procedures were performed according to the manufacturer's protocol.

2.6 Crystal violet live cell staining

After treatment for indicated time, media were removed and cells were fixed with a mixture of methanol: acetic acid (3:1) for 15 minutes at room temperature, stained with 0.5% crystal violet in 25% methanol (MeOH) for 30 minutes at room temperature, and washed with tap water. The stained cells from each well were respectively dissolved in 1% SDS and the resultant lysates were measured for their absorbance recorded at 560 nm.

2.7 RNA extraction, Reverse transcription (RT) and polymerase chain reaction (PCR)

mRNAs were extracted by TRIzol Reagent (Invitrogen). Reverse transcription was performed using SuperScript III reverse transcriptase (Invitrogen) according to the manufacturers' protocol. PCR was performed with the EconoTaq PLUS 2X Master Mix (Lucigen Corporation) on Mastercycler gradient (Eppendorf). The relative mRNA levels were determined by the Gel-Pro Analyzer program, and normalized with the reference gene 18S rRNA. The primer pairs for human FGF2: (+) 5'-CAATTCCCATGTGCTGTGAC-3' and (–) 5'-GGCAGACGAATGCCTTATGT-3', 18S rRNA: (+) 5' -GTGGAGCGATTTGTCTGGTT-3' and (–) 5'-CGCTGAGCCAGTCAGTGTAG-3' were used in the PCR reactions described above.

2.8 Trypan blue staining

After treatment for indicated time, media were removed and cells were washed with phosphate buffered saline for three times, then incubated with 0.4% trypan blue solution (HiMedia, Cat # TCL046) for 5 minutes at room temperature. The resultant cells were then fixed in 4% paraformaldehyde solution in phosphate buffered saline for counting the trypan blue stained and unstained cell numbers under microscope.

2.9 Na^+/K^+-ATPase α1 Gene Silence

The pseudotyped lentivirus containing Na^+/K^+-ATPase α1 shRNA (ATP1A1-shRNA) (clone ID:

TRCN0000332624 and TRCN0000444902) or negative control-shRNA (shLacZ, clone ID: TRCN0000231722) (Academia Sinica, Taiwan) were transduced into A549 carcinoma cells. At 24 h post transduction, the cells were cultured in the presence of 2 μg/ml puromycin for selection. The selected cells showing knockdown expression of Na^+/K^+-ATPase α1 were validated by western blot analysis and subjected to further western analysis for MKP1.

2.10 Statistical analysis

Results are reported as average values from at least three independent experiments and illustrated with average values and standard deviation (S.D.). The significance was analyzed by a 2-tailed unpaired Student's t test.

3. Results

3.1 Cardenolides induced extracellular release of FGF2 and FGFR1 phosphorylation in A549 carcinoma cells - The A549 adenocarcinoma cell line was used in this study since the FGF2 affects the A549 cell proliferation, angiogenesis, and tumor growth (He et al., 2018; Li et al., 2014). Thus, the effect of cardenolides in regulating FGF2 was studied herein in A549 cells. Treatment with ouabain or reevesioside A (Figure 1A) decreased intracellular FGF2 protein levels in proportion to dose (Figure 1B) and over time (Figure 1C), and increased the amount of FGF-2 secreted into the

culture medium (Figure 1D). Because FGF2 export was found to be decreased in transfected primate cells of COS-1 or CV-1, with expression vectors of FGF2 or α-subunit of Na^+/K^+-ATPase (Dahl et al., 2000; Florkiewicz et al., 1998), we also examined the biological function of the released FGF2. We found that FGFR1 phosphorylation increased in a dose-dependent manner and with time, while levels of the regular form of FGFR1 were diminished (Figure 1B & 1C), presumably due to endocytosis upon endocrine FGF2 binding (Wesche et al., 2011). Therefore, we conclude that the cardenolides ouabain and reevesioside A were able to promote the export of biologically functional FGF2 into culture medium, which in turn binds to FGFR1 at the cell surface, activating FGF2/FGFR1 signaling.

3.2 Cardenolides increased FGF2 transcription and proteasomal inhibition increased cardenolide-induced FGFR1 phosphorylation - Semi-quantitative RT-PCR analyses of the mRNA levels of FGF2 upon treatment with reevesioside A or ouabain were carried out at the indicated concentrations for 6 hr. (Figure 2A-a). Reevesioside A or ouabain treatment increased the transcriptional expression of FGF2 at higher doses as quantified and normalized with 18S as the internal loading control (Figure 2A-b). On the other hand, the treatment with MG132 (a proteasome inhibitor), prior to addition of reevesioside A had no significant effect on intracellular FGF2 protein levels compared to addition of reevesioside A alone, but further increased the levels of FGFR1 and its phosphorylated form (Figure 2B). Thus, it is conceivable that the cardenolide-mediated

upregulation of FGF2 transcription (Figure 2A) also contributed to the increased amounts of the exported FGF2 (Figure 1D). Furthermore, proteasomal inhibition may not contribute to FGF2 export, but was nevertheless able to slow the endocytosis of FGF2/FGFR1 complex, thus increased FGFR1 phosphorylation level and activation by cardenolides.

3.3 SU5402, an inhibitor of FGFR1, antagonized FGF2/FGFR1 activation and cardenolide-mediated cell growth inhibition – Next we used the FGFR1 inhibitor SU5042 to antagonize ouabain-induced FGFR1 phosphorylation; the results were as anticipated, in a dose dependent manner (Figure 3A)**.** Cardenolides are potent inhibitors of the growth of a variety of carcinoma cells (Chang et al., 2013b; Diederich et al., 2017; Hsiao et al., 2016). In addition, we found that ouabain and reevesioside A inhibited A549 cell grow with an IC_{50} value of 33.8 ± 4.2 nM and 50.4 ± 8.5 nM (Figure 3B-a). Since FGF2/FGFR1 signaling is involved in angiogenesis, cell growth, proliferation, and survival (Ornitz and Itoh, 2015; Raju et al., 2014; Sandhu et al., 2014), we further dissected its role in A549 cell growth. SU5402, an inhibitor of FGFR1, weakly inhibited the growth of A549 cells, with an IC_{50} value of 33.2 ± 2.4 μM (Figure 3B-a); and not only antagonized ouabain-induced FGFR1 phosphorylation (Figure 3A) but also the growth inhibition of A549 carcinoma cells by reevesioside A (Figure 3B-b).

3.4 Cardenolides promoted FGF2 export in A549 cells by activation of ERK1/2 - To elucidate

the underlying mechanisms by which the cardenolides induce FGF2 export in A549 cells, we first examined whether blockage of the unconventional route for FGF2 would affect FGF2 export (Ebert et al., 2010; Florkiewicz et al., 1998; Nickel, 2007, 2011; Nickel and Seedorf, 2008; Zacherl et al., 2015). Neither the PI3K inhibitor LY294000 nor the Tec inhibitor LFM-A13 decreased FGF2 export. As expected, the exocytosis inhibitor $MeNH_2$ (Monti et al., 2013) failed to decrease ouabain-induced FGF2 export (Figure 4A). Therefore, we proceeded to examine the effect of MAPK inhibition, since modulations of Na^+/K^+-ATPase (Haas et al., 2000; Haas et al., 2002; Ono et al., 2016; Rajamanickam et al., 2017) and FGF2/FGFR1 (Harding and Nechiporuk, 2012; van der Noll et al., 2013; Yang et al., 2008) both are able to activate downstream MAPKs. ERK1/2, JNK1/2, and p38 in A549 cells were found to be activated (phosphorylated) upon ouabain treatment and MPK1 protein levels decreased (Figure 4B). However, only the ERK1/2 inhibitor U0126 was able to significantly decrease the FGF2 export in a dose dependent manner (Figure 4C). Thus, ERK1/2 signaling plays a fundamental role in FGF2 export.

MTS and trypan blue staining were performed to clarify that the cell death or leaky cells were not associated with the reduced or increased secretion of FGF2 by different treatments. While there are increased or decreased FGF2 secretion upon different treatments (Figure 4A & C), but no significant difference in their relative cell viability were found from all co-treatments as assayed by MTS (Figure 4D-a). Moreover, trypan blue staining was utilized to look for relative dead or leaky cell numbers as shown in Figure 4D-b. Results from all the co-treatments that resulted the increased

FGF2 secretion all did not have significant change in relative cell population stained by trypan blue compared to ouabain treatment alone. The co-treatments of ouabain with U0126, which decreased the FGF2 secretion, also exhibited a decrease in the relative population of trypan blue stained cell population compared to ouabain treatment alone. This could be reasoned that U0126 reduced the secretion of FGF2 induced by ouabain and therefore decreased the subsequent endocytosis events for FGFR1, thus the uptake of trypan blue into cells (Suganuma et al., 1989) was also decreased.

3.5 Ouabain triggered EGFR-associated activation of ERK1/2, which contributed to the ERK1/2 activation for FGF2/FGFR1 activation - ERK1/2 activation triggered by cardenolide binding to the Na^+/K^+-ATPase complex was associated through the signalosome with EGFR (Haas et al., 2000; Haas et al., 2002; Ono et al., 2016; Rajamanickam et al., 2017). We found that ouabain treatment also induced phosphorylation of EGFR in addition to ERK1/2 phosphorylation. The EGFR inhibitor gefitinib was able to specifically and significantly decrease both the degree of ouabain induced ERK1/2 phosphorylation and the consequent FGFR1 phosphorylation/activation, but had no significant effect on the ouabain induced diminishment of MKP1 or the phosphorylation of JNK (Figure 5).

3.6 The MKP1 inhibitor NSC95397 mimicked the cardenolide-induced MKP1 diminishment to activate ERK1/2 phosphorylation and FGF2/FGFR1 signaling - ERK1/2 phosphorylation is

down regulated by MKP1 (Arrizabalaga et al., 2017; Cao et al., 2017). The MKP1 inhibitor NSC95397 was used to inhibit MKP1 enzymatic activity and thereby mimic cardenolide-mediated MKP1 diminishment. NSC95397 treatment increased the ERK1/2 phosphorylation in a dose dependent manner (Figure 6A) and activated the subsequent FGF2/FGFR1 signaling (Figure 6B). Moreover, depletion of Na^+/K^+-ATPase α 1 did not affect the protein level of MKP1 (Figure 6C).

Therefore, we conclude that ouabain induced FGF2 export is caused by ouabain-mediated ERK1/2 activation through EGFR activation and MKP1 diminishment. EGFR activation (Figure 5) and MKP1 diminishment (Figure 6) by ouabain were independent of each other, since the EGFR inhibitor gefitinib had no significant effect on the ouabain induced diminishment of MKP1 (Figure 5) and the diminishment of MKP1 by ouabain was not associated with Na^+/K^+-ATPase α1 (Figure 6C).

4. Discussions:

Functional Na^+/K^+-ATPase complex hydrolyzes ATP to generate energy for the exchange of two K^+ ions with three Na^+ ions. Cardenolides inhibit this process by binding to the α catalytic subunit of Na^+/K^+-ATPase, which causes it to undergo a conformation change (Agrawal et al., 2012; Diederich et al., 2017; Pavlovic, 2014). The Na^+/K^+-ATPase / cardenolide complex also forms various signalosomes which trigger a diverse range of cellular signaling pathways.

Na^+/K^+-ATPase complex is mainly associated with signalsomes in caveolae through direct interaction with caveolin, Src, PI3K etc. Several associated signalings have been reported. For

instance, Na^+/K^+-ATPase complex is coupled with Src/EGFR complex to trigger downstream signaling, e.g. ras/raf/MEK/ERK cascade(Haas et al., 2002); is associated with PI3K signalosomes, e.g. PKC-PI3K or PI3K-PDK1, with a multitude of biological consequences (Yang et al., 2018); interacts with caveolin associated cardiotonic steroid-induced signal transduction (Quintas et al., 2010). However, ouabain increased the pump activities of Na^+/K^+-ATPase complex in cells where expression of caveolin was knocked out, but was unable to activate the Src-ERK1/2 (Quintas et al., 2010) or PI3K-α -ERK1/2 (Bai et al., 2016) axes for signal transduction. Therefore, Na^+/K^+-ATPase may interact with or form different signalsomes to trigger and transduce signaling for various cellular events depending on the specific content of the cells, e.g. FGF2 export. These interplays, correlations, and the associated underlying mechanism of action remain to be uncovered.

Herein, we present the unprecedented finding that cardenolides up-regulate FGF2 export in A549 carcinoma cells, despite having been shown to down-regulate it in transfected primate cells with ectopically expressed FGF2 and Na^+/K^+-ATPase α-catalytic subunit (Dahl et al., 2000; Florkiewicz et al., 1998). We suggest that differences in the contents of the cells used may account for this differentiated regulation for FGF2 export.

Based on our findings, we conclude that cardenolide treatment triggers activation of EGFR and downregulation of MKP1 protein levels, and thereby these independent upstream signalings converge to ultimately activate ERK1/2, which significantly promotes FGF2 export. The released FGF2 in turn acts as an endocrine to bind and activate FGFR1 at the cell surface, for further

signaling cascades.

5. ACKNOWLEDGEMENTS

This work was funded by the National Health Research Institutes, Taiwan, R.O.C. and the Ministry of Science and Technology, Taiwan, R.O.C. (grants of MOST 106-2320-B-400-009-MY3, MOST 106-2811-B-400-025, MOST 107-2811-B-400-529 and MOST 108-2811-B-400-511). We also would like to acknowledge the assistance from Taiwan and National RNAi Core Facility, Academia Sinica, Taiwan.

6. AUTHOR CONTRIBUTIONS

G.H.Z. and Y.Q.Q. performed most of the biochemistry, and molecular biology experiments. C.W.Y. performed parts of the biochemistry, and molecular biology experiments. I.S.C. and C.Y.C. advised with the concept. S.J.L., G.H.Z., Y.Q.Q., and C.W.Y. participated in the design and analysis of various experiments. G.H.Z., Y.Q.Q., and S.J.L. interpreted the data and wrote the manuscript. S.J.L. supervised the experimental design, the interpretation of the data, and the composition of the manuscript.

7.CONFLICT OF INTEREST

The authors declare no conflict of interest.

8. References:

Agrawal, A.A., Petschenka, G., Bingham, R.A., Weber, M.G., Rasmann, S., 2012. Toxic cardenolides: chemical ecology and coevolution of specialized plant-herbivore interactions. The New phytologist 194, 28-45.

Arrizabalaga, O., Moreno-Cugnon, L., Auzmendi-Iriarte, J., Aldaz, P., Ibanez de Caceres, I., Garros-Regulez, L., Moncho-Amor, V., Torres-Bayona, S., Pernia, O., Pintado-Berninches, L., Carrasco-Ramirez, P., Cortes-Sempere, M., Rosas, R., Sanchez-Gomez, P., Ruiz, I., Caren, H., Pollard, S., Garcia, I., Sacido, A.A., Lovell-Badge, R., Belda-Iniesta, C., Sampron, N., Perona, R., Matheu, A., 2017. High expression of MKP1/DUSP1 counteracts glioma stem cell activity and mediates HDAC inhibitor response. Oncogenesis 6, 401.

Bai, Y., Wu, J., Li, D., Morgan, E.E., Liu, J., Zhao, X., Walsh, A., Saikumar, J., Tinkel, J., Joe, B., Gupta, R., Liu, L., 2016. Differential roles of caveolin-1 in ouabain-induced Na+/K+-ATPase cardiac signaling and contractility. Physiological genomics 48, 739-748.

Baker Bechmann, M., Rotoli, D., Morales, M., Maeso Mdel, C., Garcia Mdel, P., Avila, J., Mobasheri, A., Martin-Vasallo, P., 2016. Na,K-ATPase Isozymes in Colorectal Cancer and Liver Metastases. Front Physiol 7, 9.

Cao, T., Yang, D., Zhang, X., Wang, Y., Qiao, Z., Gao, L., Liang, Y., Yu, B., Zhang, P., 2017. FAM3D inhibits glucagon secretion via MKP1-dependent suppression of ERK1/2 signaling. Cell biology and toxicology 33, 457-466.

Chang, H.-S., Chiang, M.Y., Hsu, H.-Y., Yang, C.-W., Lin, C.-H., Lee, S.-J., Chen, I.-S., 2013a. Cytotoxic cardenolide glycosides from the root of Reevesia formosana. Phytochemistry 87, 86-95.

Chang, H.S., Chiang, M.Y., Hsu, H.Y., Yang, C.W., Lin, C.H., Lee, S.J., Chen, I.S., 2013b. Cytotoxic cardenolide glycosides from the root of Reevesia formosana. Phytochemistry 87, 86-95.

Coumoul, X., Deng, C.X., 2003. Roles of FGF receptors in mammalian development and congenital diseases. Birth defects research. Part C, Embryo today : reviews 69, 286-304.

Dahl, J.P., Binda, A., Canfield, V.A., Levenson, R., 2000. Participation of Na,K-ATPase in FGF-2 secretion: rescue of ouabain-inhibitable FGF-2 secretion by ouabain-resistant Na,K-ATPase alpha subunits. Biochemistry 39, 14877-14883.

Diederich, M., Muller, F., Cerella, C., 2017. Cardiac glycosides: From molecular targets to immunogenic cell death. Biochemical Pharmacology 125, 1-11.

Du, X., Xie, Y., Xian, C.J., Chen, L., 2012. Role of FGFs/FGFRs in skeletal development and bone regeneration. Journal of cellular physiology 227, 3731-3743.

Ebert, A.D., Laussmann, M., Wegehingel, S., Kaderali, L., Erfle, H., Reichert, J., Lechner, J., Beer, H.D., Pepperkok, R., Nickel, W., 2010. Tec-kinase-mediated phosphorylation of fibroblast growth factor 2 is essential for unconventional secretion. Traffic (Copenhagen, Denmark) 11, 813-826.

Florkiewicz, R.Z., Anchin, J., Baird, A., 1998. The inhibition of fibroblast growth factor-2 export by cardenolides implies a novel function for the catalytic subunit of Na+,K+-ATPase. The Journal of biological chemistry 273, 544-551.

Florkiewicz, R.Z., Majack, R.A., Buechler, R.D., Florkiewicz, E., 1995. Quantitative export of FGF-2 occurs through an alternative, energy-dependent, non-ER/Golgi pathway. Journal of cellular physiology 162, 388-399.

Haas, M., Askari, A., Xie, Z., 2000. Involvement of Src and epidermal growth factor receptor in the signal-transducing function of Na+/K+-ATPase. The Journal of biological chemistry 275, 27832-27837.

Haas, M., Wang, H., Tian, J., Xie, Z., 2002. Src-mediated inter-receptor cross-talk between the Na+/K+-ATPase and the epidermal growth factor receptor relays the signal from ouabain to mitogen-activated protein kinases. The Journal of biological chemistry 277, 18694-18702.

Harding, M.J., Nechiporuk, A.V., 2012. Fgfr-Ras-MAPK signaling is required for apical constriction via apical positioning of Rho-associated kinase during mechanosensory organ formation. Development (Cambridge, England) 139, 3130-3135.

He, L., Meng, Y., Zhang, Z., Liu, Y., Wang, X., 2018. Downregulation of basic fibroblast growth factor increases cisplatin sensitivity in A549 non-small cell lung cancer cells. Journal of cancer research and therapeutics 14, 1519-1524.

Hogan, B.L., Barkauskas, C.E., Chapman, H.A., Epstein, J.A., Jain, R., Hsia, C.C., Niklason, L., Calle, E., Le, A., Randell, S.H., Rock, J., Snitow, M., Krummel, M., Stripp, B.R., Vu, T., White, E.S., Whitsett, J.A., Morrisey, E.E., 2014. Repair and regeneration of the respiratory system: complexity, plasticity, and mechanisms of lung stem cell function. Cell stem cell 15, 123-138.

Hsiao, P.Y., Lee, S.J., Chen, I.S., Hsu, H.Y., Chang, H.S., 2016. Cytotoxic cardenolides and sesquiterpenoids from the fruits of Reevesia formosana. Phytochemistry 130, 282-290.

Hughes, P., Marshall, D., Reid, Y., Parkes, H., Gelber, C., 2007. The costs of using unauthenticated, over-passaged cell lines: how much more data do we need? BioTechniques 43, 575, 577-578, 581-572 passim.

Itoh, N., Ornitz, D.M., 2004. Evolution of the Fgf and Fgfr gene families. Trends in genetics : TIG 20, 563-569.

Katz, A., Tal, D.M., Heller, D., Habeck, M., Ben Zeev, E., Rabah, B., Bar Kana, Y., Marcovich, A.L., Karlish, S.J., 2015. Digoxin derivatives with selectivity for the alpha2beta3 isoform of Na,K-ATPase potently reduce intraocular pressure. Proceedings of the National Academy of Sciences of the United States of America 112, 13723-13728.

Laursen, M., Yatime, L., Nissen, P., Fedosova, N.U., 2013. Crystal structure of the high-affinity Na+K+-ATPase-ouabain complex with Mg2+ bound in the cation binding site. Proceedings of the National Academy of Sciences of the United States of America 110, 10958-10963.

Lee, K.H., Lee, C.T., Kim, Y.W., Han, S.K., Shim, Y.S., Yoo, C.G., 2005. Preheating accelerates mitogen-activated protein (MAP) kinase inactivation post-heat shock via a heat shock protein

70-mediated increase in phosphorylated MAP kinase phosphatase-1. The Journal of biological chemistry 280, 13179-13186.

Lee, Y.Z., Yang, C.W., Hsu, H.Y., Qiu, Y.Q., Yeh, T.K., Chang, H.Y., Chao, Y.S., Lee, S.J., 2012. Synthesis and biological evaluation of tylophorine-derived dibenzoquinolines as orally active agents: exploration of the role of tylophorine e ring on biological activity. Journal of medicinal chemistry 55, 10363-10377.

Li, D., Wei, X., Xie, K., Chen, K., Li, J., Fang, J., 2014. A novel decoy receptor fusion protein for FGF-2 potently inhibits tumour growth. British journal of cancer 111, 68-77.

Monti, M., Donnini, S., Morbidelli, L., Giachetti, A., Mochly-Rosen, D., Mignatti, P., Ziche, M., 2013. PKCepsilon activation promotes FGF-2 exocytosis and induces endothelial cell proliferation and sprouting. Journal of molecular and cellular cardiology 63, 107-117.

Nickel, W., 2007. Unconventional secretion: an extracellular trap for export of fibroblast growth factor 2. Journal of cell science 120, 2295-2299.

Nickel, W., 2011. The unconventional secretory machinery of fibroblast growth factor 2. Traffic (Copenhagen, Denmark) 12, 799-805.

Nickel, W., Seedorf, M., 2008. Unconventional mechanisms of protein transport to the cell surface of eukaryotic cells. Annual review of cell and developmental biology 24, 287-308.

Ono, Y., Tsuruma, K., Takata, M., Shimazawa, M., Hara, H., 2016. Glycoprotein nonmetastatic melanoma protein B extracellular fragment shows neuroprotective effects and activates the PI3K/Akt and MEK/ERK pathways via the Na+/K+-ATPase. Scientific reports 6, 23241.

Ornitz, D.M., Itoh, N., 2001. Fibroblast growth factors. Genome biology 2, REVIEWS3005.

Ornitz, D.M., Itoh, N., 2015. The Fibroblast Growth Factor signaling pathway. Wiley interdisciplinary reviews. Developmental biology 4, 215-266.

Pavlovic, D., 2014. The role of cardiotonic steroids in the pathogenesis of cardiomyopathy in chronic kidney disease. Nephron. Clinical practice 128, 11-21.

Pinilla-Macua, I., Grassart, A., Duvvuri, U., Watkins, S.C., Sorkin, A., 2017. EGF receptor signaling, phosphorylation, ubiquitylation and endocytosis in tumors in vivo. eLife 6. pii: e31993. doi: 10.7554/eLife.31993.

Qiu, Y.-Q., Yang, C.-W., Lee, Y.-Z., Yang, R.-B., Lee, C.-H., Hsu, H.-Y., Chang, C.-C., Lee, S.-J., 2015. Targeting a ribonucleoprotein complex containing the caprin-1 protein and the c-Myc mRNA suppresses tumor growth in mice: an identification of a novel oncotarget. Oncotarget 6, 2148-2163.

Quintas, L.E., Pierre, S.V., Liu, L., Bai, Y., Liu, X., Xie, Z.J., 2010. Alterations of Na+/K+-ATPase function in caveolin-1 knockout cardiac fibroblasts. Journal of molecular and cellular cardiology 49, 525-531.

Rajamanickam, G.D., Kastelic, J.P., Thundathil, J.C., 2017. The ubiquitous isoform of Na/K-ATPase (ATP1A1) regulates junctional proteins, connexin 43 and claudin 11 via Src-EGFR-ERK1/2-CREB pathway in rat Sertoli cells. Biology of reproduction 96, 456-468.

Raju, R., Palapetta, S.M., Sandhya, V.K., Sahu, A., Alipoor, A., Balakrishnan, L., Advani, J., George,

B., Kini, K.R., Geetha, N.P., Prakash, H.S., Prasad, T.S., Chang, Y.J., Chen, L., Pandey, A., Gowda, H., 2014. A Network Map of FGF-1/FGFR Signaling System. Journal of signal transduction 2014, 962962.

Sandhu, D.S., Baichoo, E., Roberts, L.R., 2014. Fibroblast growth factor signaling in liver carcinogenesis. Hepatology (Baltimore, Md.) 59, 1166-1173.

Suganuma, M., Sayama, Y., Nakamura, M., 1989. [Trypan blue staining capacities of the culture cells (2)--The mechanism of staining]. Rinsho byori. The Japanese journal of clinical pathology 37, 1361-1366.

van der Noll, R., Leijen, S., Neuteboom, G.H., Beijnen, J.H., Schellens, J.H., 2013. Effect of inhibition of the FGFR-MAPK signaling pathway on the development of ocular toxicities. Cancer treatment reviews 39, 664-672.

Wesche, J., Haglund, K., Haugsten, E.M., 2011. Fibroblast growth factors and their receptors in cancer. The Biochemical journal 437, 199-213.

Wilkie, A.O., Morriss-Kay, G.M., Jones, E.Y., Heath, J.K., 1995. Functions of fibroblast growth factors and their receptors. Current biology : CB 5, 500-507.

Yang, C.W., Chang, H.Y., Lee, Y.Z., Hsu, H.Y., Lee, S.J., 2018. The cardenolide ouabain suppresses coronaviral replication via augmenting a Na(+)/K(+)-ATPase-dependent PI3K_PDK1 axis signaling. Toxicology and applied pharmacology 356, 90-97.

Yang, H., Xia, Y., Lu, S.Q., Soong, T.W., Feng, Z.W., 2008. Basic fibroblast growth factor-induced neuronal differentiation of mouse bone marrow stromal cells requires FGFR-1, MAPK/ERK, and transcription factor AP-1. The Journal of biological chemistry 283, 5287-5295.

Zacherl, S., La Venuta, G., Muller, H.M., Wegehingel, S., Dimou, E., Sehr, P., Lewis, J.D., Erfle, H., Pepperkok, R., Nickel, W., 2015. A direct role for ATP1A1 in unconventional secretion of fibroblast growth factor 2. The Journal of biological chemistry 290, 3654-3665.

LEGENDS OF FIGURES

Figure 1. The cardenolides ouabain and reevesioside A regulate FGF2/FGFR1 in a dose- and time-dependent manner. The chemical structures of ouabain and reevesioside A (**A**). Treatment of A549 carcinoma cells with ouabain or reevesioside A decreased cellular FGF2 protein levels but increased the phosphorylation levels of its receptor FGFR1 at tyrosine 766 in proportion to dose (**B**)

and over time (**C**), while the secreted FGF-2 in the cultured medium increased (**D**). Quantification and statistical significance analysis of B-a and C-a are shown in B-b and C-b. A549 carcinoma cells were seeded and treated in RPMI-1640 medium with 1% FBS prior to western immunoblot analysis with indicated antibodies. In the dose response experiment, the cells were treated with compounds at the indicated concentration for 6 hr; in the time course experiment, the most effective doses of reevesioside A or ouabain in B was used and thus the cells were treated with vehicle (0.01 % DMSO), reevesioside A (600 nM) or ouabain (300 nM) for the indicated time in C. The enzyme-linked immunosorbent assay (ELISA; R&D Systems) was used to measure the relative extracellular FGF2 in culture supernatant upon reevesioside A or ouabain treatment (D-a) at the indicated concentration for 6 hr in RPMI-1640 medium containing 1% FBS; at the same time, crystal violet live cell staining was performed to verify the integrity of cell membrane for the duration of the analyses (D-b). The culture supernatants from A549 carcinoma cells were collected and centrifuged at 1000 g for 5 min prior to crystal violet live cell staining to remove particulates. Dimethylsulfoxide (DMSO, Sigma-Aldrich) was used as vehicle at 0.01 %. ELISA measurements for FGF2 were carried out in duplicate for each independent experiment. The results shown are representative of three independent experiments**.** Quantification shown are averages ± S.D. of 3 independent experiments A 2-tailed unpaired Student's t test was applied to estimate the significance between two group. *, $p<0.05$; **, $p<0.01$; ***, $p<0.001$. NTC, no template control.

Figure 2. Neither transcription nor proteolysis contributed to the decrease in intracellular protein levels of FGF2 upon treatment of cardenolides. A. Effects of reevesioside A or ouabain on the transcriptional expression of FGF2. Semi-quantitative RT-PCR analyses of the mRNA levels of FGF2 upon treatment with reevesioside A or ouabain at the indicated concentrations for 6 hr. **(**A-a**).** Quantification of the mRNA levels of FGF2 in EtBr (ethidium bromide)-stained agarose gels after normalization with 18S as an internal loading control by Image-J software (A-b). **B.** Effects of MG132 on intracellular FGF2 and FGFR1, upon cardenolide treatment. The pre-treatment of MG132, a proteasome inhibitor, for 0.5 hr prior to treatment with indicated concentrations of reevesioside A for another 6 hr (B-a). Semi-quantitative RT-PCR (A) or immunoblot (B) analyses were performed with indicated primer pairs or antibodies after treatment in A549 carcinoma cells in RPMI-1640 medium containing 1% FBS. The vehicle control was treatment of 0.2% DMSO for the duration of pharmacological inhibition of proteasome by MG132. The effective doses of MG132, 10 and 30 μM, were used herein. The results shown are representative of 3 independent experiments. Quantification shown are averages ± S.D of 3 independent experiments. *, $p<0.05$; **, $p<0.01$; ***, $p<0.001$.

Figure 3. SU5402, an inhibitor of FGFR1, antagonized FGFR1 activation and cell growth inhibition by cardenolides. A. SU5402 antagonized the FGFR1 phosphorylation induced by ouabain. The A549 carcinoma cells were seeded, treated and analyzed at 6 hr as described in Figure 1 prior to western immunoblot analysis with indicated antibodies. The effective doses of SU5402, 10

and 30 μM, were used to antagonize the FGFR1 phosphorylation induced by ouabain. **B.** SU5402 antagonized the cell growth inhibition by cardenolides. B-a. Growth inhibition curves of ouabain, reevesioside A, and SU5402 against A549 carcinoma cells. B-b. SU5402 antagonized the A549 cell grow inhibition by reevesioside A. The cellular responses were analyzed after compound treatment for 6 h in A and cell viability after compound treatment for three days in B. Combination index (CI) values were estimated for the drug effect of SU5402 upon the treatment of reevesioside A using CalcuSyn software (Biosoft). Both drugs were applied with a series of two-fold dilutions from the highest concentrations, 600 nM and 30 μM respectively, as in a drug ratio of 20 for the combination treatment experiment. The CI values represent the synergic, additive, or antagonistic effect of the drugs at effective doses of 50%, 75% or 90% (ED_{50}, ED_{75}, ED_{90}). Values below 0.8 are interpreted as a synergistic effect; between 0.8 and 1.2 as an additive effect; and above 1.2 as an antagonistic effect. Growth inhibition were carried out in duplicate for each independent experiment. The results shown are presentative of 3 independent experiments. Quantification shown are averages ± S.D. of 3 independent experiments. *, $p<0.05$; **, $p < 0.01$; ***, $p < 0.001$.

Figure 4. Cardenolides activated ERK1/2 to promote FGF2 export in A549 cells. A. Neither the PI3K inhibitor LY294000 nor the Tec inhibitor LFM-A13 nor the exocytosis inhibitor $MeNH_2$ decreased FGF2 export by ouabain. **B.** Ouabain activated MAPKs and diminished MKP1 protein levels. **C.** ERK1/2 inhibition by U0126 diminished the FGF2 secretion induced by ouabain. For **A** &

C, the relative extracellular FGF2 in culture supernatant was measured by an ELISA kit. A549 carcinoma cells were pre-treated with escalated doses of LY294002, $MeNH_2$, LFM-A13, U0126, SP600125 or SB203580 for 30 min and co-treated with ouabain for 6 hr in 1% FBS RPMI-1640 medium. The culture supernatants were collected and cell debris were removed by centrifugation at 1000 g for 5 min. For **B**, A549 cells were incubated with reevesioside A or ouabain for 6 hr before sample collection for followed western analysis with the indicated antibodies. ELISA measurements for FGF2 were carried out in duplicate for each independent experiment. **D**. MTS and trypan blue staining for cells from different co-treatments. MTS and trypan blue staining were performed to clarify that the cell death or leaky cells were not associated with the reduced or increased secretion of FGF2 by different treatments for 6 hr as in **A** and **C**. MTS and Trypan blue staining experiments were carried out in duplicate for each independent experiment. The results shown are representative of 3 independent experiments. Quantification shown are averages ± S.D. of 3 independent experiments, and each in duplicate for A & C . The two-tailed unpaired Student's t test was used for statistical analyses. *, $p < 0.05$; **, $p < 0.01$; ***, $p < 0.001$.

Figure 5. The EGFR inhibitor gefitinib decreased ouabain-induced activation of EGFR and downstream activation of ERK 1/2 but not JNK 1/2. A549 cells were pre-treated with gefitinib for 30 min and then treated with ouabain for the indicated time in 1% FBS RPMI-1640 medium. Pretreatment of 20 μM gefitinib (an effective dose for inhibiting EGFR phosphorylation) in A549

cells diminished ouabain-induced activation and phosphorylation of EGFR, ERK and FGFR1, but had no effect either on MKP1 protein levels nor JNK activation. The results shown are representative of 3 independent experiments. Quantification shown are averages ± S.D. of 3 independent experiments. The two-tailed unpaired Student's t test was used for statistical analyses. *, $p < 0.05$; **, $p < 0.01$; ***, $p < 0.001$. ns, not significant.

Figure 6. MKP1 inhibition by NSC95397 resembled ouabain-induced activation of ERK1/2 and FGF2/FGFR1. A. ERK1/2 were phosphorylated in response to MKP1 inhibition by NSC95397 in a dose-dependent manner. A549 cells were incubated with indicated concentrations of NSC95397 for 6 hr in 1% FBS RPMI-1640 medium. One of effective doses of NSC95397 (50 μM) in A was chosen for the followed experiment in B. **B.** NSC95397 and ouabain both mediated FGFR1 phosphorylation and degradation. A549 cells were treated with NSC95397 or ouabain for 4, 5 and 6 hr in 1% FBS RPMI-1640 medium prior to western immunoblot analysis. The results shown are representative of 3 independent experiments. C. Knockdown of Na^+/K^+-ATPase α1 expression did not affect the MKP1 protein level. Na^+/K^+-ATPase α1 is denoted ATP1A1. Validated knocked down cells were seeded onto a 6 well-plate, 8×10^5 cells/well, and cultured for 24 h prior to harvesting for western analysis with the antibodies indicated. Quantification shown are averages ± S.D. of 3 independent experiments. The two-tailed unpaired Student's t test was used for statistical analyses. *, $p < 0.05$; **, $p < 0.01$; ***, $p < 0.001$.

Figure 7. Illustrative scheme for the cardenolides induced converging Erk1/2 activation for promoting FGF2 export and FGFR activation.

November-18-2019

"BCP_D-19-01245"

AUTHOR CONTRIBUTIONS

G.H.Z. and Y.Q.Q. performed most of the biochemistry, and molecular biology experiments. C.W.Y. performed parts of the biochemistry, and molecular biology experiments. I.S.C. and C.Y.C. advised with the concept. S.J.L., G.H.Z., Y.Q.Q., and C.W.Y. participated in the design and analysis of various experiments. G.H.Z., Y.Q.Q., and S.J.L. interpreted the data and wrote the manuscript. S.J.L. supervised the experimental design, the interpretation of the data, and the composition of the manuscript.

November-18-2019 "BCP_D-19-01245"

Highlights:

5) Cardenolides induced FGF2 secretion and FGFR1 phosphorylation in A549 cells.
6) Cardenolide ouabain triggered the EGFR associated ERK 1/2 activation.
7) Cardenolide ouabain diminished the MKP1 protein level and thus resulted in ERK 1/2 activation.
8) Cardenolides induced converged ERK1/2 activation to promote the FGF2 export in A549 cells.

1

2

3